(Received 22 November 2023, Accepted 12 February 2024, Scheduled 22 March 2024)

High-Performance Silicon Nitride Grating-Coupled SPR Sensors for Gas Detection and Biosensing

Mounir Bouras*

Laboratoire d'Analyse des Signaux et Systèmes, Département d'Electronique
Université Mohamed Boudiaf - M'Sila, BP. 166, Route Ichebilia, M'sila 28000, Algeria

ABSTRACT: Surface Plasmon Resonance (SPR) serves as a crucial optical technique in the realm of chemical sensing. Under specific conditions, the reflectivity of a thin metal film exhibits an exceptional sensitivity to optical changes in the medium on one side. In this investigation, we propose and simulate a plasmonic sensor incorporating a silicon nitride grating with Ag layers for the detection of solution and gas at an optical communication wavelength of 1550 nm. In both cases of the surface diffraction-grating, there is a notable enhancement in angular sensitivity compared to conventional prism-coupled configurations. Simulations, employing rigorous coupled wave analysis (RCWA), highlight that the suggested sensor, optimized in design parameters, offers notably superior sensitivity, a lower detection limit, and a higher figure of merit (FOM) than existing grating-based SPR sensors. This implies the potential realization of refractive index sensors with a high figure of merit through such streamlined and compact configurations.

1. INTRODUCTION

Throughout history, the miniaturization of transistors has played a pivotal role in propelling the semiconductor industry's development, especially concerning advanced nanofabrication facilities. These well-established technologies have not only shaped the semiconductor landscape but also facilitated the downsizing of nanostructures in organic materials, allowing for high-resolution and cost-effective patterning for plasmonic sensor applications. In contemporary times, advanced organic materials nanostructures are commonly produced using nanoimprint lithography technique [1]. Additionally, within nanostructures, the interaction of light and matter can be effectively manipulated at the nanoscale by combining organic materials nanostructures with semiconductors, organic metallic elements, and biomolecules [2]. Engineered metallic nanostructures have been successfully applied in various domains, including plasmonic antennas [3], biosensing [4], molecular fingerprints [5], thermoplasmonic desalination [6, 7], plasma-wave photodetectors [8], minerals recovery [9], optics [10], catalysis [11, 12], energy production [13], and imaging [14].

The predominant technology for surface wave resonance-based sensing is SPR method [15]. This approach operates by inducing surface plasmon polaritons along a metal/dielectric interface through incident light. However, a limitation of SPR is its excitation exclusively by TM light, and the presence of strong dispersion in the metal components invariably leads to absorption. Typically, the sensitivity of SPR biosensors is on the order of several tens of degrees per refractive index unit (°/RIU) [16, 17].

In the realm of sensing, SPR has been extensively investigated for environmental monitoring, medical diagnostics, and sensing and detection over the last three decades or so [3]. It is crucial to highlight that the direct optical excitation of SPR on a slick metal surface is not feasible, necessitating the incorporation of suitable light coupling schemes for surface plasmons generation.

As a potential alternative, SPR can be combined with nanostructures [18–21], where a thin metal film is combined with periodic corrugations at subwavelength scales. This alternative approach offers notable advantages in terms of high-throughput, ease of integration, and miniaturization. Furthermore, the resonance characteristics of surface plasmons can be finely tuned in organic materials nanostructures by optimizing grating variables such as groove depth, duty cycle, and period.

Photonic Integrated Circuits (PICs) are poised to play a pivotal role in the development of efficient and user-friendly integrated spectrometers and sensors. Silicon nitride (Si_3N_4) emerges as a versatile High-Index-Contrast (HIC) platform, offering transparency across both visible and infrared wavelengths [22]. Its compatibility with the well-established complementary-metal-oxide-semiconductor (CMOS) process technology positions Si_3N_4 as an ideal candidate for the realization of low-cost photonic devices, akin to the achievements in silicon photonics.

The novelty of this study is rooted in the utilization of a silicon nitride (Si_3N_4) grating and a thin Ag layer in conjunction with a SPR based sensor for the sensitive detection of bio-solutions and gases. The strategic choice of the wavelength (1550 nm) aligns with the refractive index (RI) range of 1.330–1.350 for the bio-solution layer and 1–1.006 for the gases layer. This correspondence outlines the design of a single-mode Si_3N_4 strip waveguide optimized for the 1550 nm wavelength. The culmination of this effort is the inaugural demonstration of Grating Couplers in the near-infrared (NIR) spectrum (1200–1400 nm) specifically tailored for Si_3N_4 waveguides. The fo-

* Corresponding author: Mounir Bouras (mounir.bouras@univ-msila.dz).

cus of this presentation is on elucidating the coupling efficiency and its intricate dependencies on wavelength, incident angle, and the etch depth of the grating. This property qualifies the proposed structure well-suited for on-chip applications dedicated to controlling variations in bio-analytes and gases.

Our research capitalizes on the NIR spectral region, offering distinct advantages in biosensing. This region reduces signal scattering, particularly Rayleigh scattering, in comparison to visible wavelengths. The evaluation of our proposed grating sensor centers on sensitivity and the figure of merit (FOM) value. We delve into the impact of grating variables and the thickness of the Ag layer on the sensor's performance, considering both logical and practically feasible design considerations. Furthermore, we conduct a comparative analysis, pitting the performance of our proposed grating SPR sensor against previously reported noteworthy works that employ grating nanostructures in SPR sensors. This approach provides valuable insights into the advancements and efficacy of our proposed sensor within the broader context of existing research in the field.

2. SENSOR DESIGN AND THEORETICAL BACKGROUND

2.1. Sensor Design

The suggested structure for a grating-based (SPR) sensor is depicted in Fig. 1.

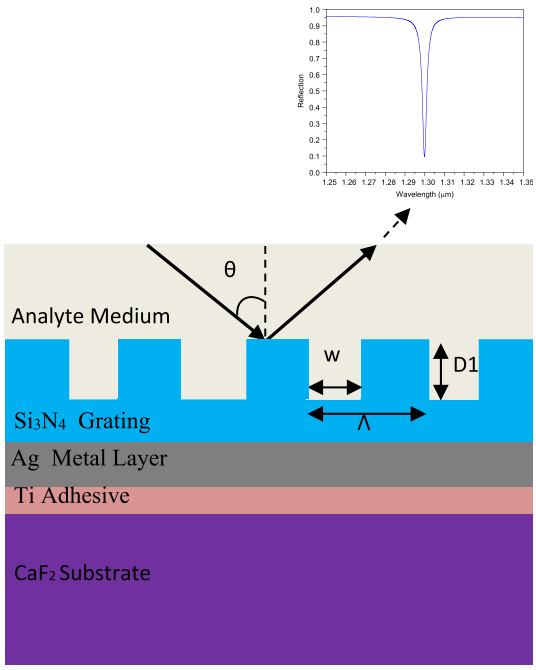

FIGURE 1. Schematic diagrams of grating-coupled (SPR) sensor. Additionally, reflectivity curve versus wavelength is shown on the above.

The chosen substrate material for the sensor is CaF_2, a fluoride glass, selected for its advantages in the NIR spectral region [23]. Over this substrate, a 2 nm thick titanium (Ti) film is applied as an adhesive layer between CaF_2 and the subsequent Metal layer [24]. Silver is chosen for its active role in plasmonic applications, featuring high optical conductivity. Notably, the real and imaginary parts of Ag's dielectric constant remain constant within the range of 25 nm–50 nm thickness [11], making it suitable for the intended purpose.

To construct the surface diffraction-grating sensor, a grating layer of (Si_3N_4) is deposited above the Ag layer. This surface diffraction-grating layer is specifically designed to couple propagating illuminations with the SPR mode. In Fig. 1, the fundamental structure of a standard 1D binary rectangular grating is illustrated, featuring the period 'Λ,' groove depth '$D1$', and duty cycle 'w'. The grating period (Λ) in the structure adheres to the Bragg condition, expressed as $\Lambda = 2\lambda_0/N_{eff}$. Here, N_{eff} denotes the real part of the effective index of the waveguide, and λ_0 represents the incident wavelength in a vacuum. The duty cycle is set to half of the grating period. Notably, the groove depth and profile emerge as critical parameters in the design of the grating, and a detailed discussion on these aspects will follow.

2.2. Theory and Performance Parameters

Several widely employed methods for modeling nanostructure devices encompass finite-difference time-domain (FDTD) [13], finite element method (FEM) [25], rigorous-coupled wave analysis (RCWA) [26], and non-equilibrium Green's function method [27]. Both FDTD and FEM methods involve the discretization of the structure for effective modeling. In contrast, RCWA stands apart as it does not necessitate discretization. As a semi-analytical method, RCWA demands less computation time than techniques like FDTD and FEM. Therefore, structures featuring extremely small geometries can be conveniently modeled using RCWA.

The RCWA method has been chosen for several reasons. Firstly, it addresses Maxwell's equations through fully vectorial calculations without resorting to any approximation. Additionally, the effective medium theory is generally suitable when the feature size is significantly smaller than the considered wavelengths. However, it has been previously reported that RCWA performs effectively across a wide range of grating period to wavelength ratios [28].

Given these considerations, the RCWA method was deemed appropriate for this study. The calculations described herein were conducted using Diffract MOD, integrated into the RSoft Photonics Suite. Diffract MOD, based on the RCWA method [23, 26], incorporates advanced algorithms with Fourier harmonics designed to describe periodic dielectric functions.

In the context of a grating-coupled surface plasmon resonance sensor, it is generally favorable to have a low diffraction order and a larger grating period. This configuration is sought after to attain notably high sensitivity [27]. The resonance wavelength (λ_{SPR}), corresponding to R_{min} (minimum reflectivity), is a crucial parameter. The fundamental SPR sensing principle relies on the fact that even a slight change in analyte properties, such as refractive index (RI), induces a shift in the position of λ_{SPR}.

It is worth noting that in dielectric grating-based structures, like the one employed in this study, two dips generally appear — one corresponding to the substrate mode and the other to the

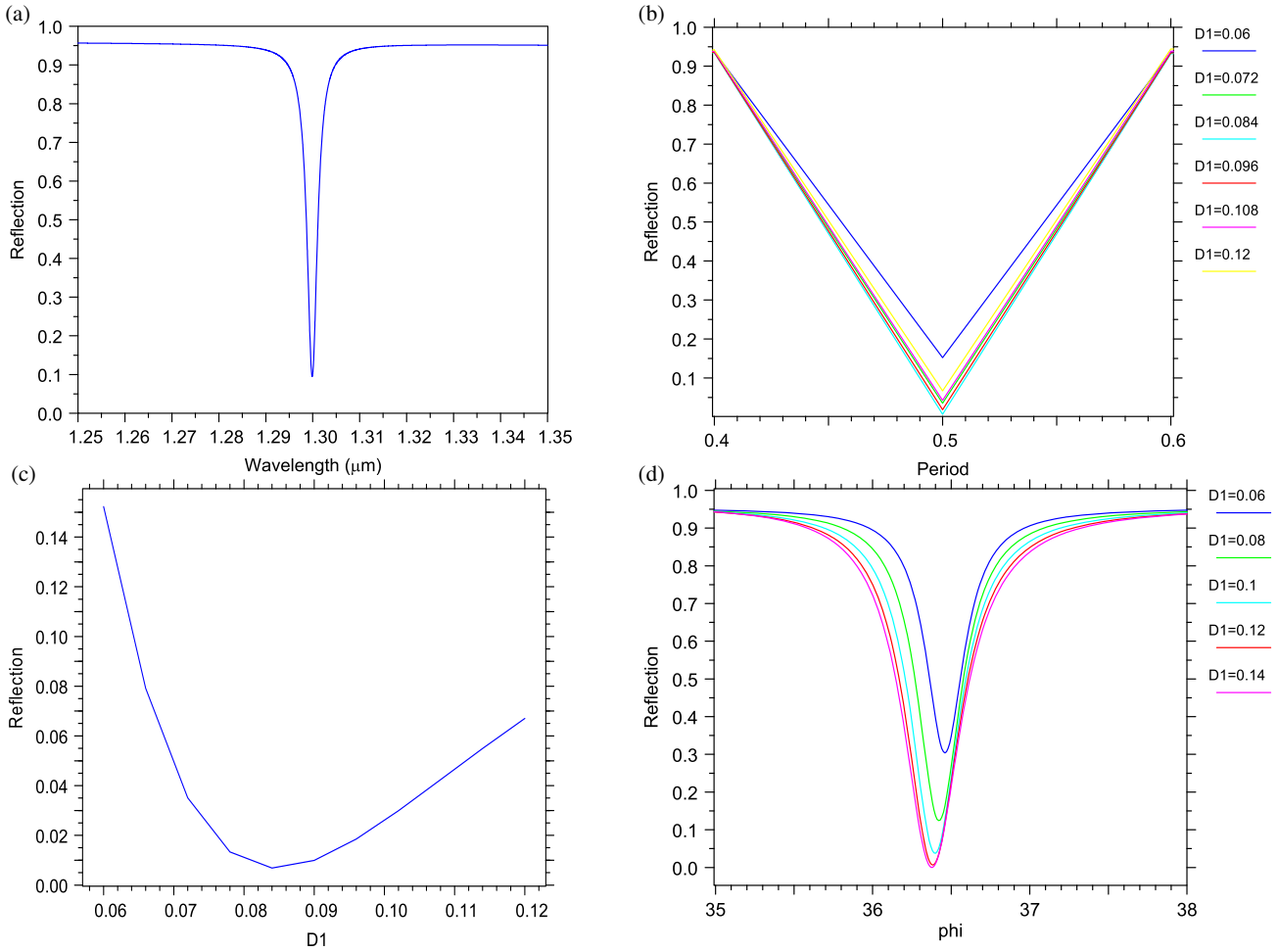

FIGURE 2. Reflectance spectra (based on RCWA method) SPR curves with (a) wavelength, (b) period, (c) depth $D1$, (d) incident angles ϕ.

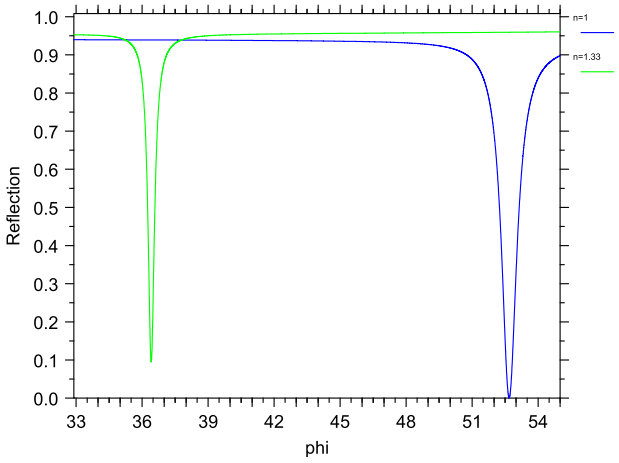

FIGURE 3. Reflectance spectra as a function of incident angles ϕ for the analyte of air and water.

plasmon mode. The wavelength linked to the substrate mode dip tends to remain nearly constant, while the one tied to the plasmon mode dip varies with changes in analyte properties. The substrate mode dip can serve as a reference, allowing for the development of self-referenced SPR sensors, as previously reported [28]. However, in scenarios involving variations in analyte properties, such as changes in water concentration or gas in this study, the alteration in the SPR dip alone is sufficient for sensing purposes. This is facilitated by considering the reference Water with a refractive index of 1.33 and assigning a value of 1 for Air.

The crucial performance metrics for SPR-based sensors include sensitivity (S) and figure of merit (FOM). Sensitivity is defined as the ratio of the corresponding shift in resonance wavelength ($\Delta\lambda_{\text{SPR}}$) to a small change in refractive index (Δn_s) of the sensing medium, expressed as $= \Delta\lambda_{\text{SPR}}/\Delta n_s$.

Figure of merit (FOM) is another important sensor performance indicator. FOM can be improved in the RI sensor by decreasing FWHM, increasing the spectral sensitivity S [°/RIU], or both, as FOM$\propto$S/FWHM. The FOM of many optical sensors is constrained by an intrinsic trade-off between spectral sensitivity and FWHM.

3. RESULTS AND DISCUSSION

The focus of this paper is on the discussion of reflectivity at resonance angle (Rc), full width at half maximum (FWHM), and sensitivity of a Silicon Nitride Grating-based Plasmonic Refractive Index Sensor with varying groove depths. All sim-

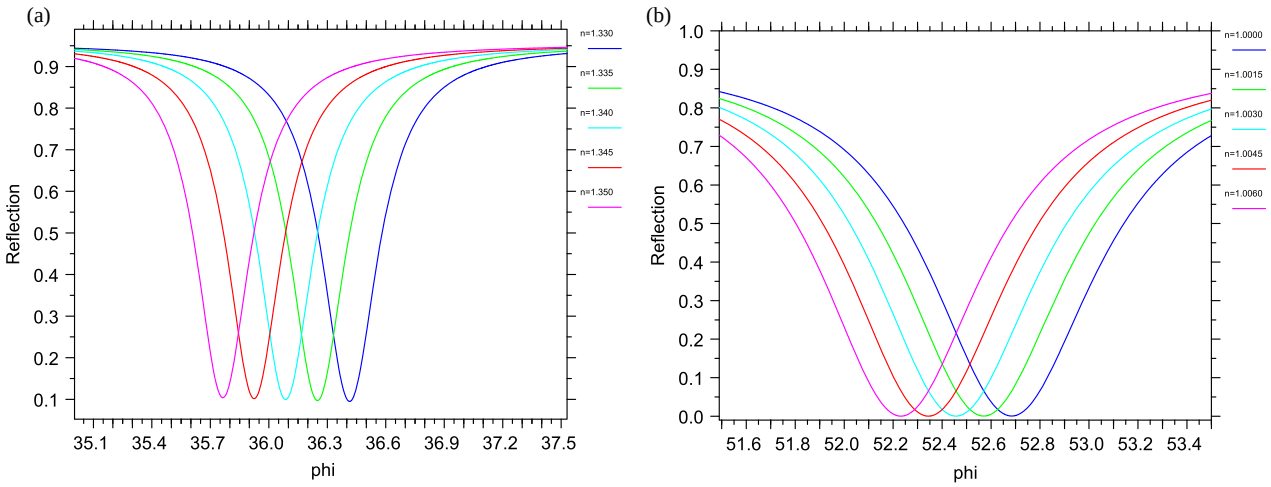

FIGURE 4. Reflectivity curves as a function of incident angles ϕ.

ulations were conducted at an incident light wavelength of $\lambda_0 = 1550\,\text{nm}$.

In plasmonic structures, changes in the refractive index of the surrounding medium (analyte) can have a significant impact on the intensity of reflected light. Plasmonics involves the interaction between electromagnetic waves and surface plasmons, which are collective oscillations of electrons at the interface between a metal and a dielectric. Surface Plasmon Resonance (SPR) occurs when the frequency of incident light matches the natural frequency of surface plasmons, leading to a strong enhancement of the electromagnetic field at the metal-dielectric interface. The interaction between incident light and surface plasmons creates an enhanced evanescent field at the metal-dielectric interface. Changes in the refractive index of the analyte influence the penetration depth and strength of this evanescent field, affecting the intensity of reflected light.

Figure 2 illustrates simulated SPR curves for various groove depths at an incident angle (ϕ) of 36.4°, representing normal light incidence on the grating structure. The corresponding reflectivity spectra for groove depths of 60 nm, 72 nm, 84 nm, 96 nm, 108 nm, and 120 nm are shown in Figs. 2(b), (c), and (d).

The results clearly illustrate that the groove depth, a parameter controlled during fabrication, significantly influences the grating transmittance. It can be adjusted to achieve the desired transmittance values. The optimized set of design parameters is identified as follows: groove depth $(Dl) = 84\,\text{nm}$, duty cycle $(w) = 500\,\text{nm}$, and period $(\Lambda) = 970\,\text{nm}$, leading to a large quality factor (QF). Importantly, the performance of the proposed structure surpasses that of previously reported works on grating-based plasmonic sensors.

An increase in the refractive index of the analyte typically leads to a redshift (toward longer wavelengths) of the SPR resonance, while a decrease in refractive index results in a blueshift (toward shorter wavelengths). This shift is associated with changes in the optical properties of the plasmonic structure, influencing the reflected light intensity. Fig. 3 displays reflectivity curves for these modes as a function of the angle of incidence. Sharp resonance features are evident in both bio-solution and gas cases as a function of angle incidence. In the water solution, a distinct dip peak emerges at $\phi = 36.5°$ with incident angle interrogation, while for the air analyte, the resonant angle is $\phi = 52.7°$. The optimization of device parameters can enhance the quality factor of the resonant peak.

Figure 4 illustrates the reflectivity curves as a function of incident angle (ϕ) for various refractive index values. In both cases, when the refractive index undergoes a uniform change, the SPR peaks exhibit a blue shift. This means that even a slight alteration in the refractive index value ($\Delta n_{\text{bio-sol}} = 0.005$ and $\Delta n_{\text{gas}} = 0.0015$) results in an increased angle shift between the resonance peaks, particularly at small incident angles.

Table 1 presents a comparison of the sensing characteristics for the two cases, evaluating sensitivity and FWHM as functions of the surrounding refractive index. The analysis revealed a consistent increase in both sensitivity and FWHM with heightened variations in biomolecule concentrations. Notably, the sensitivity in the gases case was approximately twice that of the bio-solution case, while the resonances exhibited narrower FWHM values in gases than bio-solution.

TABLE 1. Calculated parameters for two cases proposed.

CASES	FWHM (nm)	S (°/RIU)	FOM (1/RIU)
Bio-solution	0.4	36	90
Gases	0.8	84	105

In our study, the sensitivity reached 36°/RIU for the bio-solution case and 84°/RIU for gas. This suggests that the bio-solution sensor exhibits a closer overlap between the resonant mode and the sensing layer than the gas sensor. Notably, the sensitivity of both SPR configurations tested is an order of magnitude higher than that of the conventional prism-based scheme (refer to Table 2). Unlike biosensor designs based on prism-coupled excitation, there is no strict refractive index limit for the dielectric composite used in the bio-solution or gases configurations. By appropriately scaling the parameters of the 1D grating and Ag, the proposed sensor configurations can be effectively implemented in any wavelength range.

TABLE 2. Comparison of material, and sensitivity of proposed structure with other sensors in literature.

Reference	Material	Sensitivity
[23]	Ta_2O_5/SiO_2	18°/RIU (Experimental)
[29]	Si/SiO_2	27°/RIU
[26, 27]	Porous silicon	72°/RIU
[22]	Chalcogenide	128°/RIU
This work		36°/RIU (For Bio-solution)
		84°/RIU (For Gas)

4. CONCLUSIONS

In this Work, we delved into surface diffraction 1D grating configurations and their applications in sensing. A schematic for a surface diffraction-grating configuration was designed based on the rigorous coupled-wave analysis (RCWA) methodology. The optimized gases biosensor exhibited a notably large increase in sensitivity (two-fold) and a narrower surface plasmon resonance (SPR) than bio-solution sensor. Both 1D-grating-coupled sensor platforms examined in this study displayed a lower quality factor than traditional sensors. However, the quality factor could be potentially enhanced by fine-tuning parameters such as the period (Λ) and grating depth (D). The proposed configurations for exciting SPR in both bio-solution and gases represent a new class of compact setups for highly sensitive biosensing. They hold promise for the development of nanoscale "lab-on-chip" technologies in the future.

REFERENCES

[1] Chen, J., J. Shi, D. Decanini, E. Cambril, Y. Chen, and A.-M. Haghiri-Gosnet, "Gold nanohole arrays for biochemical sensing fabricated by soft UV nanoimprint lithography," *Microelectronic Engineering*, Vol. 86, No. 4-6, 632–635, 2009.

[2] Lindquist, N. C., P. Nagpal, K. M. McPeak, D. J. Norris, and S.-H. Oh, "Engineering metallic nanostructures for plasmonics and nanophotonics," *Reports on Progress in Physics*, Vol. 75, No. 3, 036501, Mar. 2012.

[3] Sadeghi, P., K. Wu, T. Rindzevicius, A. Boisen, and S. Schmid, "Fabrication and characterization of Au dimer antennas on glass pillars with enhanced plasmonic response," *Nanophotonics*, Vol. 7, No. 2, 497–505, 2017.

[4] Lopez, G. A., M.-C. Esteve, M. Soler, and L. M. Lechuga, "Recent advances in nanoplasmonic biosensors: Applications and lab-on-a-chip integration," *Nanophotonics*, Vol. 6, No. 1, 123–136, Jan. 2017.

[5] Badri, S. H., M. M. Gilarlue, S. S. Nahaei, and J. S. Kim, "High-Q Fano resonance in all-dielectric metasurfaces for molecular fingerprint detection," *Journal of the Optical Society of America B*, Vol. 39, No. 2, 563–569, 2022.

[6] Santoro, S., A. H. Avci, A. Politano, and E. Curcio, "The advent of thermoplasmonic membrane distillation," *Chemical Society Reviews*, Vol. 51, 6087–6125, 2022.

[7] Abramovich, S., D. Dutta, C. Rizza, S. Santoro, M. Aquino, A. Cupolillo, J. Occhiuzzi, M. F. L. Russa, B. Ghosh, D. Farias, A. Locatelli, D. W. Boukhvalov, A. Agarwal, E. Curcio, M. B. Sadan, and A. Politano, "NiSe and CoSe topological nodal-line semimetals: A sustainable platform for efficient thermoplasmonics and solar-driven photothermal membrane distillation," *Small*, Vol. 18, No. 31, 2201473, Aug. 2022.

[8] Viti, L., J. Hu, D. Coquillat, A. Politano, W. Knap, and M. S. Vitiello, "Efficient terahertz detection in black-phosphorus nanotransistors with selective and controllable plasma-wave, bolometric and thermoelectric response," *Scientific Reports*, Vol. 6, 20474, Feb. 2016.

[9] Santoro, S., M. Aquino, C. Rizza, A. Cupolillo, D. W. Boukhvalov, G. D'Olimpio, S. Abramovich, A. Agarwal, M. B. Sadan, A. Politano, and E. Curcio, "Plasmonic nanofillers-enabled solar membrane crystallization for mineral recovery," *Desalination*, Vol. 563, 116730, Oct. 2023.

[10] Dutta, D., B. Ghosh, B. Singh, H. Lin, A. Politano, A. Bansil, and A. Agarwal, "Collective plasmonic modes in the chiral multifold fermionic material CoSi," *Physical Review B*, Vol. 105, 165104, Apr. 2022.

[11] Politano, A. and G. Chiarello, "The influence of electron confinement, quantum size effects, and film morphology on the dispersion and the damping of plasmonic modes in Ag and Au thin films," *Progress in Surface Science*, Vol. 90, No. 2, 144–193, May 2015.

[12] Chiarello, G., J. Hofmann, Z. Li, V. Fabio, L. Guo, X. Chen, S. D. Sarma, and A. Politano, "Tunable surface plasmons in Weyl semimetals TaAs and NbAs," *Physical Review B*, Vol. 99, 121401, Mar. 2019.

[13] Avci, A. H., S. Santoro, A. Politano, M. Propato, M. Micieli, M. Aquino, Z. Wenjuan, and E. Curcio, "Photothermal sweeping gas membrane distillation and reverse electrodialysis for light-to-heat-to-power conversion," *Chemical Engineering and Processing — Process Intensification*, Vol. 164, 108382, Jul. 2021.

[14] Park, K.-D. and M. B. Raschke, "Polarization control with plasmonic antenna tips: A universal approach to optical nanocrystallography and vector-field imaging," *Nano Letters*, Vol. 18, No. 5, 2912–2917, 2018.

[15] Nishi, H., S. Hiroya, and T. Tatsuma, "Potential-scanning localized surface plasmon resonance sensor," *ACS Nano*, Vol. 9, No. 6, 6214–6221, Jun. 2015.

[16] Masson, J.-F., "Surface plasmon resonance clinical biosensors for medical diagnostics," *ACS sensors*, Vol. 2, No. 1, 16–30, 2017.

[17] Michel, D., F. Xiao, and K. Alameh, "A compact, flexible fiber-optic surface plasmon resonance sensor with changeable sensor chips," *Sensors and Actuators B: Chemical*, Vol. 246, 258–261, Jul. 2017.

[18] Raether, H., *Surface Plasmons on Smooth and Rough Surfaces and on Gratings*, Vol. 111, Springer-Verlag, Berlin, Heidelberg, New York, 1988.

[19] Pandey, A. K., A. K. Sharma, and R. Basu, "Fluoride glass-based surface plasmon resonance sensor in infrared region: Performance evaluation," *Journal of Physics D: Applied Physics*, Vol. 50, No. 18, 185 103(1–6), 2017.

[20] Mounir, B., C. Haouari, A. Saïd, and A. Hocini, "Analysis of highly sensitive biosensor for glucose based on a one-dimensional photonic crystal nanocavity," *Optical Engineering*, Vol. 58, No. 2, 027102, 2019.

[21] Charik, H., M. Bouras, and H. Bennacer, "High-sensitive thermal sensor based on a 1D photonic crystal microcavity with nematic liquid crystal," *Progress In Electromagnetics Research M*, Vol. 100, 187–195, 2021.

[22] Gorin, A., A. Jaouad, E. Grondin, V. Aimez, and P. Charette, "Fabrication of silicon nitride waveguides for visible-light using PECVD: A study of the effect of plasma frequency on optical properties," *Optics Express*, Vol. 16, No. 18, 13 509–13 516, 2008.

[23] Valsecchi, C. and A. G. Brolo, "Periodic metallic nanostructures as plasmonic chemical sensors," *Langmuir*, Vol. 29, No. 19, 5638–5649, 2013.

[24] Pandey, A. K. and A. K. Sharma, "Simulation and analysis of plasmonic sensor in NIR with fluoride glass and graphene layer," *Photonics and Nanostructures - Fundamentals and Applications*, Vol. 28, 94–99, Feb. 2018.

[25] Johnson, P. B. and R. W. Christy, "Optical constants of the noble metals," *Physical Review B*, Vol. 6, No. 12, 4370–4379, 1972.

[26] Moharam, M. G. and T. K. Gaylord, "Rigorous coupled-wave analysis of planar-grating diffraction," *Journal of the Optical Society of America*, Vol. 71, No. 7, 811–818, 1981.

[27] Moharam, M. G., E. B. Grann, D. A. Pommet, and T. K. Gaylord, "Formulation for stable and efficient implementation of the rigorous coupled-wave analysis of binary gratings," *Journal of the Optical Society of America A*, Vol. 12, No. 5, 1068–1076, 1995.

[28] Mirotznik, M. S., B. L. Good, P. Ransom, D. Wikner, and J. N. Mait, "Broadband antireflective properties of inverse motheye surfaces," *IEEE Transactions on Antennas and Propagation*, Vol. 58, No. 9, 2969–2980, Sep. 2010.

[29] Zhao, B., "Thermal radiative properties of micro/nanostructured plasmonic metamaterials including two-dimensional materials," Georgia Institute of Technology, 2016.